Impulsive Eruptive Flare on 23 October, 2003, from NOAA AR 10484

Cristiani G.[1], Mandrini C.H.[1], Nuevo F.[1], Chandra R.[2], Joshi B.[3], Schmieder B.[4], Uddin W.[5]

(1) Instituto de Astronomía y Física del Espacio / CONICET-UBA Buenos Aires, Argentina **(2)** Department of Physics-Kumaun University, Nainital, Uttarakhand, India
(3) Udaipur Solar Observatory, Udaipur, India **(4)** Observatoire de Paris, Meudon, Paris, France **(5)** Aryabhatta Research Institute of Observational Sciences, Nainital, Uttarakhand, India

Abstract

We present and discuss the multi-wavelength observations of an M2.4 flare that occurred in active region NOAA 10484 on 23 October, 2003. The flare was well observed by ARIES Hα Solar Tower Telescope, TRACE, SOHO, and RHESSI instruments. The flare was very impulsive and eruptive in nature, accompanied by a narrow coronal mass ejection (CME). Hα and TRACE observations show that initially the jet is ejected in the east direction. We observe X-ray compact sources at the flare location. These 50-100 keV sources coincide with TRACE bright kernels and may indicate the locations of the footpoints of reconnected loops. The flare site is a region of mixed field sign, where emergence of new polarities together with moving magnetic features (MMFs), are seen o the east of a large decaying sunspot. A local linear force-free model of AR 10484 indicates that the AR magnetic field structure consists of largescale, very extended loops and very small-scale loops, related to the new emerging flux and MMFs. These define a topological structure with two bald-patches (BPs) located at the flare site. The large-scale field lines, associated to the BPs, could represent open loops. This is confirmed by a global potential field source surface (PFSS) model, which shows that field lines rooted at the east of the AR reach the SS at 2.5 $R_\odot$. We propose that magnetic reconnection, ocurring at chromospheric level in the BP separatrices, may drive the flare and accompaying jet plasma expulsion, which later expands to give the narrow CME at the eastern solar limb.

Introduction

Under typical coronal conditions the magnetic field is force free and frozen into the plasma. Separatrix surfaces or separatrices are an exception where current layers may be formed, which can only appear in a magnetic volume when some field lines are tangentially touching the boundary (i.e. the photosphere). This can happen along portions of the inversion line for the component of the magnetic field normal to this boundary. These portions are the so-called "bald patches" or BPs [Titov *et al.*, 1993], that define separatrices where current layers can develop (see e.g. Aly & Amari, 1997). BPs are thought to be the locations where chromospheric material can be lifted up and, so, they can be also linked to processes occurring in prominences [Aulanier & Demoulin, 1998].
There are several reports that the jets can lead the CME in the outer corona [Shen *et al.*, 2012]. Occasionally impulsive flares can also be associated with such jets and CMEs. Now the question arises: How the compact or impulsive flare can generate the jet? How this jet can lead CME? what should be the magnetic configuration in the active region to generate the CME from impulsive flare and associated jets? These are the key question to understand the impulsive flares and their association to jets and CMEs.

Hα observations

The Hα evolution of the flare on 23 October, 2003 is shown in Fig. 1. In Hα the flare initiated around 02:30 UT, peaked around 02:37 UT and decayed around 02:50 UT. Similar to X-ray wavebands, the flare shows impulsive nature in Hα. The flare was initiated with the ejection of dark material (i.e. surge) in the east direction afterwards it was followed by bright mass ejection (i.e. jet) at the eastern edge of the active region. Superposing Hα images to magnetic filed contours from the closest in time MDI magnetogran we inferred that K1, K2 are in negative polarity while the kernel K3 is in positive polarity respectively.

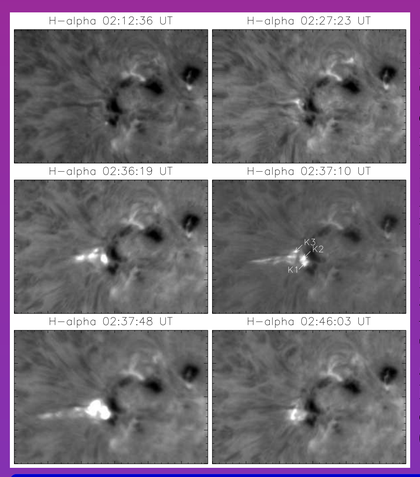

FIGURE 1: Evolution of the flare in Hα. The field-of-view of the images is 290"×200". Initially kernels K1 and K2 appear as a single bright patch. As the flare progresses, K1 and K2 become visible separately. The jet ended around 02:39 UT, however the flare continues up to 02:50 UT.

LASCO observations

The flare studied here is associated with the CME also in the same east direction. The speed of CME was 656 km sec^{-1}. It is a narrow CME having angular width of 46°, which becomes visible in the LASCO C2 field of view at 03:06 UT. Backward extrapolation of LASCO height-time plot indicates that the approximate start time of CME on the solar surface was 02:34 UT, which is consistent with the initiation time of the bright and confined plasma ejection (jet) from the flaring region. Therefore, we conjecture that the jet is closely associated with the observed CME at 03:06 UT.

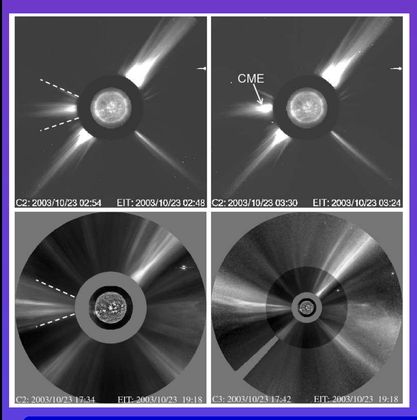

FIGURE 2: LASCO C2 and C3 images before, during and after the associated CME, to see the outer AR coronal magnetic field structure in the east direction. The CME evolution shows a persistent structure extending from the east limb at a similar latitude to that of the active region.

RHESSI observations

Fig.3 shows a sequence of TRACE 1700 Å images overlaid by RHESSI X-ray images. We find that the low energy emission (i.e., 10-15 keV) originates from a single compact source from the very beginning (∼02:33 UT) until the end of flare at ∼02:48 UT. However, in 50-100 keV energy band two HXR sources are observed for a brief period at ∼02:39 UT, which are cospatial with the northern most and southern most UV flare kernels.

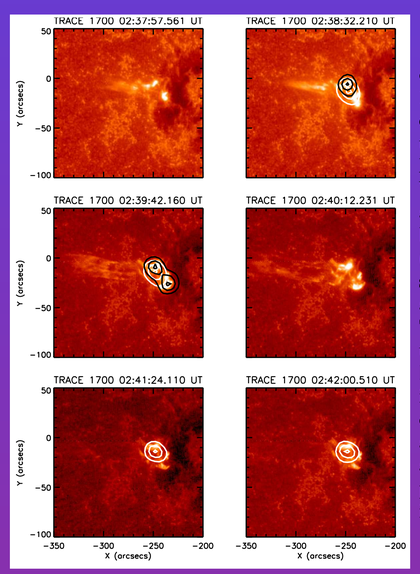

FIGURE 3: Sequence of TRACE 1700 Å images overlaid by co-temporal RHESSI X-ray images. White contours are 10-15 keV; black contours (in the first and second panels) are 50-100 keV. The integration time for each RHESSI images is 1 minute. The contour levels are 40%, 70%, and 95% of the peak flux in each image.

We examined the polarity of the X-ray sources by overploting the X-ray sources on the MDI magnetogram resulting that the two high energy HXR footpoints were located in the opposite polarity.

Magnetic field model and topology

The line-of-sight magnetic field of the AR is extrapolated using the linear force free field (LFFF) approximation: $\vec{\nabla}\times\vec{B} = \alpha\vec{B}$, where $\vec{B}$ is the magnetic field and α, called the force free parameter, is assumed to be constant in the entire extrapolation box. As a boundary condition for the model, we used the SoHO/MDI magnetogram closest in time (01:35 UT) to the observed flare. The only free parameter on which the LFFF model depends on, α, is chosen so that the computed field lines match observed coronal loops. We select to compare computed field lines to observed loops a 171 Å TRACE image. $\alpha = -1.9\times10^{-3}$ Mm^{-1} is the value that best match TRACE loops.

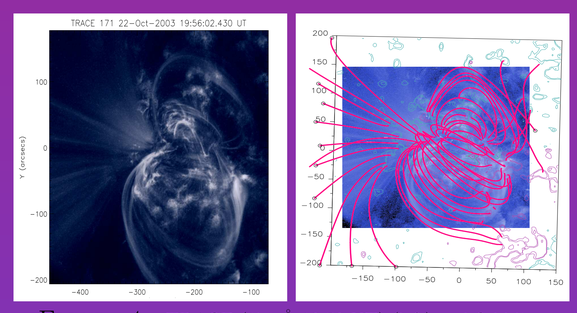

FIGURE 4: TRACE (171 Å 19:58 UT) (left) and field lines tracing the observed loops (right) overlaid on the same image. The contours correspond to ±50 G, ±100 G, and ±500 G (red for positive and cyan for negative polarities, axes are in Mm).

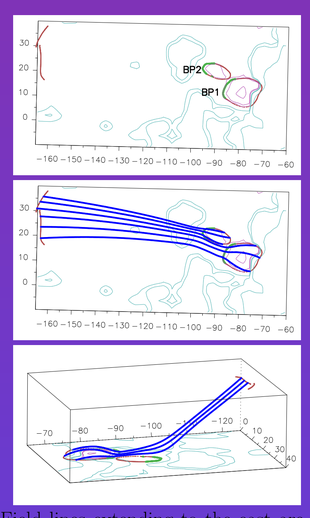

FIGURE 5: Magnetic field model showing the location of two BPs and associated field lines. In the upper panel the BPs, labeled as BP1 and BP2, are shown as thick green continuous lines at the photospheric level while the red thin continuous lines correspond to the trace of the BP separatrices. The one to the west of the two small positive polarities lies on the photospheric plane, while the one to the east is shown projected on the photosphere. The central panel shows a set of field lines starting at the phostospheric level from both sides of the BPs and reaching both separatrices traces.

Field lines extending to the east are large-scale "open" lines in our computation (i.e., they reach the limits of the computation box). The lower panel clearly shows that the separatrix to the east is not at the photosphere, but at the top of the drawn box. The height of the box is 50 Mm in this figure. For clarity we are only showing field lines from BP1 in this panel, similar field-line tracing is found for BP2. Contours are the same as in Fig. 4 and the axes are in Mm.

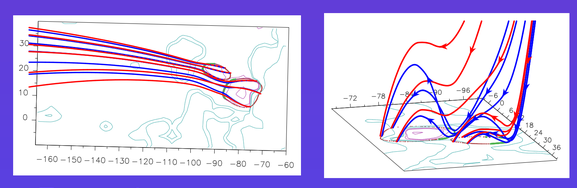

FIGURE 6: Magnetic field model showing the two BPs and a set of pre-reconnected and pos-reconnected field lines. The blue continuous lines, same set as in Fig. 5 for BP1, would correspond to the situation before reconnection, while the set of red continuous lines issued from the separatrix located at the photospheric level would correspond to the lines after reconnection. Notice that both sets extend to the east and, in fact, they are "open" lines (i.e., they reach the limits of the computation box) in our computation. The panel to the left corresponds to the observers point of view, while the panel to the right has been drawn from a different perspective in order that the field connectivity be clear. We have also added arrows to the computed lines to indicate the direction of the magnetic field. The conventions for the field isocontours, axes, BPs, and separatrices are the same as in Fig. 5.

To examine what is the magnetic field configuration from the AR towards the east limb in the large scale, we use a global Potential Field Source Surface (PFSS) model. The model is computed with the Finite Difference Iterative Potential-field Solver code developed by Toth et al. (2011), which provides more accurate results at high latitude region than are typically obtained with spherical harmonic expansion methods. The SS is set to 2.5 $R_\odot$ and the grid is spherical with 150 bins in the radial direction, 180 latitudinal bins, and 360 longitudinal bins. From Fig. 7 it is clear that there is a set of "open" field lines anchored at the east of the AR that could channel the plasma ejected during the flare that could be later seen as the narrow eastern CME depicted in Fig. 2.

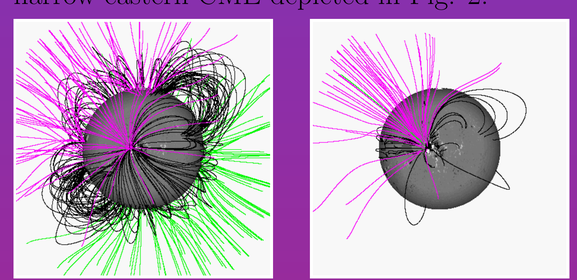

FIGURE 7: PFSS extrapolation model: left: global field model, right: local view centered in the active region.The field-line colour convention is such that black indicates closed lines and pink (green) corresponds to open lines anchored in the negative-polarity (positive-polarity) field.

Conclusion

The flare is very impulsive and associated with a jet followed by a narrow CME. The open field structure in the east side chanalised the ejected jet material in the east direction. This structure can be seen using the LASCO CME data and further it is confirmed by the PFSS and local field extrapolations. At the bottom of the ejected jet, two strong Hα and UV kernels were observed. These kernels were associated with strong high energy RHESSI X-ray sources (50-100 keV). In the RHESSI observations along with the strong footpoints, we also observed the loop-top. Initially the RHESSI 50-100 keV source is single and compact. It is interesting to note that two strong RHESSI footpoints were observed, when the jet reached its maximum height. It indicates that the reconnection is maximum when the jet reached the maximum height.
It is indeed clear from the magnetic field extrapolation that the jet is driven along the open field lines. However, the question arises about its driver. On the first instance, in the observed scenario, it seems that the magnetic reconnection between low-lying closed-field lines and large-scale open-field lines power the jet. If the height of the energy release site is less (greater) than a critical height then the jet will be driven by slow MHD mode/shocks, directly by the pressure gradient force generated by reconnection generated energy [Shibata *et al.*, 1982]. However, this minimum critical height in the solar atmosphere depends upon the strength of pressure enhancement in time at the energy release site. For the larger pressure enhancement, this height will be lower and vice versa. It is clear from the TRACE images that the surge base lies almost 10-15 Mm high compared to the forming regions of three kernels that represent the footpoints of the low-lying and localized loop-systems undergoing in the reconnection. Although, this estimation is crude as well as in the projection, however, it can provide the clues about the direct role of the magnetic reconnection. Therefore, the jet can be driven by the direct reconnection generated forces along the open field lines in upward corona.
In conclusion, we observe an impulsive flare, associated jet formed by the reconnection driven forces, as well as later its expansion in form of a narrow CME. The generation of compact HXR energy sources at the footpoints of the flaring loops univoquely combines the scenario of the most transients activities (a jet with the height of 60 Mm and a narrow but speeedy CME moving outwards, compact and impulsive flare and downward moving high energy particles) in the light of standard reconnection scenario.

References

[Aly & Amari, 1997] Aly, J. J., & Amari, T. 1997. Current sheets in two-dimensional potential magnetic fields. III. Formation in complex topology configurations and application to coronal heating. *A&A*, **319**(Mar.), 699–719.

[Aulanier & Demoulin, 1998] Aulanier, G., & Demoulin, P. 1998. 3-D magnetic configurations supporting prominences. I. The natural presence of lateral feet. *A&A*, **329**(Jan.), 1125–1137.

[Shen *et al.*, 2012] Shen, Y., Liu, Y., Su, J., & Deng, Y. 2012. On a Coronal Blowout Jet: The First Observation of a Simultaneously Produced Bubble-like CME and a Jet-like CME in a Solar Event. *ApJ*, **745**(Feb.), 164.

[Shibata *et al.*, 1982] Shibata, K., Nishikawa, T., Kitai, R., & Suematsu, Y. 1982. Numerical hydrodynamics of the jet phenomena in the solar atmosphere. II - Surges. *Sol. Phys.*, **77**(Apr.), 121–151.

[Titov *et al.*, 1993] Titov, V. S., Priest, E. R., & Demoulin, P. 1993. Conditions for the appearance of "bald patches" at the solar surface. *A&A*, **276**(Sept.), 564.

[Tóth *et al.*, 2011] Tóth, G., van der Holst, B., & Huang, Z. 2011. Obtaining Potential Field Solutions with Spherical Harmonics and Finite Differences. *ApJ*, **732**(May), 102.

57MA Reunión Anual de la Asociación Argentina de Astronomía
15 - 19 de Septiembre de 2014, Ciudad de Córdoba, Argentina